

6-2007

# The Transcriptional Repressor K-RBP Modulates RTA-Mediated Transactivation and Lytic Replication of Kaposi's Sarcoma-Associated Herpesvirus

Zhilong Yang

*University of Nebraska - Lincoln*

Charles Wood

*University of Nebraska - Lincoln, cwood1@unl.edu*

Follow this and additional works at: <http://digitalcommons.unl.edu/virologypub>



Part of the [Virology Commons](#)

---

Yang, Zhilong and Wood, Charles, "The Transcriptional Repressor K-RBP Modulates RTA-Mediated Transactivation and Lytic Replication of Kaposi's Sarcoma-Associated Herpesvirus" (2007). *Virology Papers*. 132.

<http://digitalcommons.unl.edu/virologypub/132>

This Article is brought to you for free and open access by the Virology, Nebraska Center for at DigitalCommons@University of Nebraska - Lincoln. It has been accepted for inclusion in Virology Papers by an authorized administrator of DigitalCommons@University of Nebraska - Lincoln.

# The Transcriptional Repressor K-RBP Modulates RTA-Mediated Transactivation and Lytic Replication of Kaposi's Sarcoma-Associated Herpesvirus<sup>∇</sup>

Zhilong Yang and Charles Wood\*

*Nebraska Center for Virology and School of Biological Sciences, University of Nebraska, Lincoln, Nebraska 68588*

Received 30 November 2006/Accepted 26 March 2007

**The replication and transcription activator (RTA) protein of Kaposi's sarcoma (KS)-associated herpesvirus (KSHV)/human herpesvirus 8 functions as the key regulator to induce KSHV lytic replication from latency through activation of the lytic cascade of KSHV. Elucidation of the host factors involved in RTA-mediated transcriptional activation is pivotal for understanding the transition between viral latency and lytic replication. KSHV-RTA binding protein (K-RBP) was previously isolated as a cellular RTA binding protein of unknown function. Sequence analysis showed that K-RBP contains a Kruppel-associated box (KRAB) at the N terminus and 12 adjacent zinc finger motifs. In similarity to other KRAB-containing zinc finger proteins, K-RBP is a transcriptional repressor. Mutational analysis revealed that the KRAB domain is responsible for the transcriptional suppression activity of this protein and that the repression is histone deacetylase independent. K-RBP was found to repress RTA-mediated transactivation and interact with TIF1 $\beta$  (transcription intermediary factor 1 $\beta$ ), a common corepressor of KRAB-containing protein, to synergize with K-RBP in repression. Overexpression and knockdown experiment results suggest that K-RBP is a suppressor of RTA-mediated KSHV reactivation. Our findings suggest that the KRAB-containing zinc finger protein K-RBP can suppress RTA-mediated transactivation and KSHV lytic replication and that KSHV utilizes this protein as a regulator to maintain a balance between latency and lytic replication.**

Kaposi's sarcoma (KS)-associated herpesvirus (KSHV), also referred to as human herpesvirus 8, belongs to the  $\gamma$ -2 herpesvirus family (9). KSHV can establish latent infection in infected cells and can be reactivated to lytic replication (23, 62). The KSHV replication and transcription activator (RTA), encoded by KSHV immediately-early gene open reading frame 50 (ORF50), is both sufficient and necessary to induce KSHV lytic replication from latency through activation of the lytic gene expression cascade (15, 43, 70). RTA strongly activates expression of many KSHV lytic genes, including polyadenylated nuclear (PAN) RNA, ORFK8, ORF57, viral G protein-coupled receptor, vIRF1, K1, gB, and itself (4, 10, 36, 41, 42, 65, 70, 79, 88). Although the nature of the detailed mechanism of RTA-mediated transactivation is unclear, evidence suggests that various cellular factors play important roles in RTA-mediated transactivation. Several factors such as RBP-J $\kappa$ /CBF1, STAT3, CBP (CREB-binding protein), C/EBP $\alpha$ , histone deacetylase complex (HDAC), SWI/SNF, and IRF-7 have been found to associate with RTA and modulate its transcriptional activity (16–18, 32, 61, 78, 81, 85).

Our laboratory previously identified a KSHV-RTA binding protein (K-RBP) by use of a yeast two-hybrid screening of a B-cell cDNA library (80). This cellular protein, referred to as the human hypothetical protein MGC2663 or ZnF426, is encoded on human chromosome 19 (19p13.2; GenBank accession number AC008567). K-RBP expression could be detected

in several primate cell lines, including BC-3, BJAB, 293, and CV-1 cells (80). Coimmunoprecipitation and pull-down assays have further demonstrated that K-RBP interacts with RTA both in vivo and in vitro (80). K-RBP is 554 amino acids (aa) in size and displays sequence similarity to members of the Kruppel-associated box (KRAB)-containing zinc finger proteins, suggesting that K-RBP is a member of the KRAB-containing zinc finger protein family of transcriptional modulators.

KRAB-containing zinc finger proteins make up the largest single family of transcriptional regulators in mammalian cells (3). All KRAB-containing zinc finger proteins contain one or two KRAB domains located near the N terminus and 4 to 30 C<sub>2</sub>H<sub>2</sub> zinc-finger motifs at the C terminus (3, 58). The KRAB domain has been shown to be a protein-protein interaction module and a transcriptional repression domain. It contains conserved boxes known as A and/or B (b) and/or C boxes, with each KRAB domain between 50 and 75 aa in length (3, 37, 38, 45, 73). The KRAB-A box contains the transcriptional repression activity, while the B and C boxes are dispensable for repression (1, 38, 44, 77). The repression by KRAB domain has been shown to depend on the physical interaction with a protein known as TIF1 $\beta$  (transcription intermediary factor 1 $\beta$ )/KAP1 (KRAB-associated protein-1)/KRIP-1 (KRAB-A interacting protein) (12, 26, 48). TIF1 $\beta$  functions as corepressor and enhances KRAB-mediated repression. The repression activity of a KRAB-containing protein/TIF1 $\beta$  complex at the DNA regulatory region was shown to be a result of the recruitment of cellular factors to the transcriptional complex. These factors include heterochromatin protein 1 (HP1) family, a family of nonhistone heterochromatin-associated proteins with gene-silencing function, HDAC, and SETDB1, a SET domain-containing protein that methylates lysine 9 of histone H3 (30,

\* Corresponding author. Mailing address: Nebraska Center for Virology and School of Biological Sciences, University of Nebraska, E249 Beadle Center, P.O. Box 880666, Lincoln, NE 68588-0666. Phone: (402) 472-4550. Fax: (402) 472-8722. E-mail: cwood1@unl.edu.

<sup>∇</sup> Published ahead of print on 4 April 2007.

52, 56, 59, 63, 64). Due to the repression activity of KRAB domain, most of the characterized KRAB-containing zinc finger proteins such as ZBRK1, SZF1, and KS1 have been demonstrated to function as transcriptional repressors (14, 57, 87). Their function by binding to specific DNA sequences through their zinc finger motifs and mediating transcriptional repression through the KRAB domain (37, 82). Studies have also shown that KRAB-containing proteins can repress transcription indirectly via interacting with other proteins. For example, retinoblastoma (RB)-associated KRAB protein, RbAK, has been shown to interact with RB to repress E2F-dependent gene expression and inhibit DNA synthesis (67). Krim-1B (KRAB box protein interacting with Myc-1B) has been shown to interact with c-Myc and repress c-Myc-dependent transcriptional activation (20). VHL (Von Hippel-Lindau)-associated KRAB-A domain-containing protein (VHLAK) has been shown to interact with VHL and repress HIF-1 $\alpha$  (hypoxia-inducible factor-1 $\alpha$ )-mediated transcriptional activity (31).

Recently, a number of studies have shown that KRAB-containing zinc finger proteins play important roles in cell differentiation and organ development, including in bone, heart, sperm, and hematopoietic cells, and regulate their physiological processes even though the targeted genes directly controlled by KRAB-containing zinc finger proteins have not been found (21, 24, 39, 72, 84). For example, the KRAB-containing zinc finger protein AJ18 was found to be involved in bone development (24). In addition, several studies have shown that KRAB-containing zinc finger proteins are involved in regulating viral replication and transcription. ZBRK1, along with its corepressor TIF1 $\beta$ , was found to interact with the Epstein-Barr virus replication protein BBLF2/3, and this complex provides an origin-tethering function for Epstein-Barr virus replication (34). Another KRAB-containing zinc finger protein, OTK18, was found to be a human immunodeficiency virus type 1-inducible transcriptional suppressor and to suppress human immunodeficiency virus type 1 replication (7, 8). These findings indicate that KRAB-containing zinc finger proteins have diverse functions in regulating different cellular activities and virus-cell interactions through direct binding to the promoters of the target genes or indirectly by interacting with other proteins.

To understand the normal cellular function of K-RBP and its role in RTA-mediated transcriptional activation and KSHV lytic replication, we further characterized K-RBP. We demonstrated that this putative KRAB-containing zinc finger protein exhibits transcriptional repression function and interacts with the corepressor TIF1 $\beta$ . Moreover, we found that K-RBP can modulate RTA-mediated transcriptional activation and suppress KSHV reactivation from latency. These findings suggest that K-RBP, the KRAB-containing transcriptional repressor, is involved in the modulation of KSHV-RTA activity and plays a role in maintaining the balance between latency and lytic replication of KSHV.

#### MATERIALS AND METHODS

**Plasmids.** All clones with inserts that were amplified by PCR were confirmed by DNA sequence analysis. RTA expression plasmid pCMV-Tag50, which encodes a Flag-tagged RTA, was described previously (79, 80). K-RBP expression plasmids pcDNAK-RBP (pcDNA-MGC2663), which encodes the full-length human MGC2663 cDNA, and pHAK-RBP (pHA-MGC2663), which encodes a

hemagglutinin (HA)-tagged K-RBP, were also described previously (80). pHAK-RBP1-213 and pHAK-RBP214-554, deletion clones of K-RBP encoding HA-tagged K-RBP segments from aa 1 to 213 and aa 214 to 554, respectively, were constructed by inserting the corresponding DNA fragments into the mammalian expression vector pCMVHA (Clontech). Reporter plasmids p57Pluc1 and pK8Pluc, containing PCR-cloned promoter regions of KSHV ORF57 (from nucleotide [nt] 81556 to 82008) and ORFK8 (from nt 73851 to 74849), were described elsewhere (80). Reporter plasmid pPANPluc contains the promoter region of PAN RNA (from nt 28461 to 28681) inserted into the upstream portion of the luciferase reporter gene of pGL3-Basic vector (Promega). The  $\beta$ -galactosidase ( $\beta$ -Gal) expression plasmid pCMV- $\beta$  (Clontech) was used for the normalization of transfection efficiency.

The Matchmaker two-hybrid system 3 vectors used in yeast two-hybrid assay were purchased from Clontech. The constructs pGBKK-RBP, pGBKK-RBP42-98, pGBKK-RBP1-213, and pGBKK-RBP214-554, which encode full-length K-RBP and aa 42 to 98, aa 1 to 213, and aa 214 to 554 of K-RBP fused to GAL4 DNA-binding domain (GAL4BD), respectively, were generated by inserting the corresponding DNA fragments into pGBKT7 vector, which encodes the yeast GAL4 N-terminal 147-aa DNA binding domain located upstream of the inserted DNA. The yeast expression plasmid pGADTIF1 $\beta$ , which encodes TIF1 $\beta$  fused to a GAL4 activation domain, was generated by inserting the DNA fragment into pGADT7. The expression clone pCMVTIF1 $\beta$ Flag encoding the TIF1 $\beta$  was obtained from Walter Schaffner (Universität Zürich, Zürich, Switzerland) (48). pGADTIF1 $\beta$ 1-423 and pGADTIF1 $\beta$ 442-835, which encode TIF1 $\beta$  aa 1 to 423 and aa 442 to 835 fused to GAL4AD, were subcloned from pGADTIF1 $\beta$  by use of suitable restriction sites. Clones pHATIF1 $\beta$ , pHATIF1 $\beta$ 1-423, and pHATIF1 $\beta$ 442-835 encode HA-tagged TIF1 $\beta$  and the deletion mutants. The corresponding DNA fragments of TIF1 $\beta$  were obtained from pGADTIF1 $\beta$  and inserted into pCMVHA vector. The expression plasmids pHACBP, which encodes HA-tagged CBP, and pCMV $\beta$ p300, which encodes p300, were kind gifts from Clinton Jones (University of Nebraska, Lincoln, NE).

The mammalian pCMVBD vector (Stratagene) was used in GAL4BD fusion protein/GAL4-luciferase reporter assays to determine the transcriptional activity of K-RBP. The mammalian GAL4BD fused expression clones pBDK-RBP, pBDK-RBP42-98, pBDK-RBP1-213, pBDK-RBP99-213, and pBDK-RBP99-554 encode full-length K-RBP and aa 42 to 98, aa 1 to 213, aa 99 to 213, and aa 99 to 554 of K-RBP, respectively. They were generated by cloning the corresponding DNA fragments into the pCMVBD vector. Clone pBDKRX1KRAB, which encodes aa 1 to 90 of the KOX1 KRAB domain, was a kind gift from Frank J. Rauscher III (University of Pennsylvania, Philadelphia, PA) (55). The reporter plasmid pFR-luc, which contains five copies of GAL4 binding element located upstream of a firefly luciferase reporter gene, was purchased from Stratagene.

**Antibodies.** K-RBP antibody was prepared by immunizing a rabbit with *Escherichia coli*-expressed recombinant K-RBP, and the RTA antibody was prepared by immunizing a rabbit with baculovirus-expressed recombinant RTA from insect cells (Lampire Biological Laboratories). The rabbit anti-TIF1 $\beta$  polyclonal antibody was purchased from Santa Cruz Biotechnology. The mouse anti- $\gamma$ -tubulin monoclonal antibody was purchased from Sigma. The mouse anti-Flag M2 monoclonal antibody was purchased from Stratagene. The rabbit anti-HA polyclonal antibody and mouse anti-His monoclonal antibody were purchased from Clontech. The rat anti-LANA monoclonal antibody was purchased from Advanced Biotechnologies Inc. The mouse anti-K8 monoclonal antibody was purchased from Novus Biologicals. The mouse anti-K8.1 monoclonal antibody was obtained from Bala Chandran (Rosalind Franklin University, Chicago, IL).

**Yeast two-hybrid assay.** The yeast two-hybrid assay was performed using Matchmaker two-hybrid system 3 (Clontech). K-RBP and its truncated mutants were fused to the GAL4BD of the pGBKT7 plasmid. The TIF1 $\beta$  and its mutants were fused to the GAL4AD of the pGADT7 plasmid as described above. *Saccharomyces cerevisiae* AH109 was used as the reporter host strain.

**Cell culture, transfection, and luciferase assays.** Human 293T cells were grown in Dulbecco's modified Eagle medium (DMEM, Gibco BRL) supplemented with 10% fetal bovine serum (FBS; Gibco BRL) and 100  $\mu$ g/ml penicillin-streptomycin (Mediatech) at 37°C with 5% CO<sub>2</sub>. In each well of a six-well plate, 3  $\times$  10<sup>5</sup> 293T cells were transfected with 1 to 2  $\mu$ g of total DNA mixed with 2  $\mu$ l of Lipofectamine reagent (Invitrogen) in DMEM according to the manufacturer's recommendations. The total DNA amount used in each transfection was normalized by adding control plasmids. Fresh DMEM containing penicillin-streptomycin and supplemented with 20% FBS was added to the transfected cells at 7 h posttransfection, and cells were grown for an additional 17 h. Luciferase activities were determined by use of a Luciferase assay system (Promega) according to the manufacturer's procedure. Data were averaged from the results of multiple transfections performed in at least three independent experiments. The

transfection efficiency for each experiment was normalized by cotransfecting  $\beta$ -Gal expression plasmid pCMV- $\beta$  as the internal control.

Stealth small interfering RNA (siRNA) was designed using Invitrogen's BLOCK iT RNAi Designer. The sequences of siRNA targeting K-RBP are located at positions 1462 to 1486 (GenBank accession number BC001791) as follows: sense, GCCUUUGCAGUUUCCUCAAUUCUUA; and antisense, UAAGAUUUGAGGAAACUGCAAAGGC. The sequences of siRNA targeting TIF1 $\beta$  are located at positions 740 to 764 (GenBank accession number NM\_005762) as follows: sense, CAGUGCUGCACUAGCUGUGAGGAUA; and antisense, UAUCCUCACAGUAGUGCAGCAGUG. The control siRNA sequences used were as follows: sense, GGCGUCAUCCGACAGUUUUAU; and antisense, AUAACAUAACUGUCGGAUUGACGCC. Transfection of siRNA into 293T cells was conducted using Lipofectamine 2000 (Invitrogen) according to the manufacturer's procedure.

BCBL-1 is a KSHV-positive primary effusion lymphoma cell line. TRExBCBL-1RTA is a BCBL-1 cell line carrying a tetracycline-(or doxycycline-) inducible RTA gene (50) and was provided by Jae Jung (Harvard Medical School, Boston, MA). This cell line was maintained in RPMI 1640 (Gibco BRL) containing 10% FBS, 100  $\mu$ g/ml penicillin-streptomycin, and 200  $\mu$ g/ml hygromycin B at 37°C with 5% CO<sub>2</sub>. The transfection of TRExBCBL-1RTA cells was carried out using a Nucleofector device (Amaxa) according to the manufacturer's procedure. The transfection efficiency in TRExBCBL1RTA cells was found to be around 50% using this method.

Vero cells infected by rKSHV.219 virus were provided by Jeffrey Vieira (University of Washington, Seattle, WA) (76). The cells were maintained in DMEM supplemented with 10% FBS, 100  $\mu$ g/ml streptomycin-penicillin, 2 mM L-glutamine, and 5  $\mu$ g/ml puromycin in a humidified incubator at 37°C with 5% CO<sub>2</sub>. A recombinant baculovirus expressing the KSHV-RTA was also obtained from Jeffrey Vieira, and its use in the generation of rKSHV.219 virus was carried out as described earlier (76). Transfection of K-RBP siRNA into Vero cells infected with rKSHV.219 was conducted using Lipofectamine 2000 (Invitrogen) according to the manufacturer's procedure, and the transfection was carried out two times within 24 h to obtain efficient knockdown.

**Coimmunoprecipitation.** 293T cells were transfected with various combinations of expression plasmids. At 48 h posttransfection, the cells were lysed in 0.5 ml ice-cold immunoprecipitation (IP) buffer (1% Nonidet P-40, 0.5% sodium deoxycholate, and 1 mM phenylmethylsulfonyl fluoride in phosphate-buffered saline). After centrifugation at 16,000  $\times$  g for 10 min, the cell lysates were precipitated with 2 to 3  $\mu$ g of specific antibodies and incubated overnight at 4°C. Protein G beads (Amersham) (20  $\mu$ l) were then added and incubated for 2 h. The beads were then washed four times with IP buffer. The immunoprecipitated proteins were heated in sample buffer, analyzed by 7 to 10% sodium dodecyl sulfate-polyacrylamide gel electrophoresis (SDS-PAGE), and transferred to a polyvinylidene difluoride membrane (Amersham) for Western blot analysis.

**Western blot analysis.** The transferred polyvinylidene difluoride membrane was blocked with 3 to 5% nonfat dry milk in TBST (50 mM Tris [pH 7.5], 200 mM NaCl, 0.05% Tween 20) at room temperature for 1 h. It was then incubated with the primary antibody in the same TBST buffer containing milk for 1 h at room temperature. The membrane was washed three times with TBST for 10 to 15 min each time, incubated with horseradish peroxidase-conjugated secondary antibody at room temperature for 1 h, washed three times with TBST, treated with SuperSignal detection reagents (Pierce), and then exposed to Kodak light film.

**RNA extraction and RT-PCR.** Total cellular RNA was prepared using an RNeasy kit (QIAGEN) according to the manufacturer's procedure. Total RNA (1  $\mu$ g) was used for reverse transcription (RT) using oligo(dT) as a primer, and the reverse-transcribed products were then used as templates for PCR amplification with gene-specific primers.

**PCR analysis of virus progeny.** The supernatant of Vero cells infected with rKSHV.219 was collected after RTA induction and centrifuged at 2,000 rpm to spin down cell debris. The supernatant was then collected, and the viral particles were concentrated through a 20% sucrose gradient at 17,000 rpm and 4°C for 2 h. Virus pellets were resuspended in 200  $\mu$ l of 0.2 $\times$  phosphate-buffered saline, digested by DNase I for 1 h at 37°C to remove exogenous DNA, and heated to 95°C for 15 min and then 56°C for 1 h with proteinase K treatment (100  $\mu$ g/ml). The enzyme was inactivated by treatment at 95°C for 30 min; the DNA was then purified by use of a QIAGEN PCR purification kit and eluted by elution buffer. Viral DNA solution (1  $\mu$ l) was used for PCR amplification of the KSHV-specific fragment located in ORF26, and the amplicon was analyzed using 1.5% agarose gel. Real-time PCR was performed according to the manufacturer's protocol using TaqMan chemistry (Applied Biosystems). The relative amounts of DNA were calculated using Bio-Rad iCycler software (version 3.1; Bio-Rad Laboratories).

**Protein stability analysis.** For the analysis of the protein stability, approximately  $3 \times 10^6$  293T cells were transfected with plasmids expressing different proteins of interest in the presence of 75  $\mu$ g/ml cycloheximide (Sigma) for 24 h after transfection. The transfected cells were harvested at various time points after cycloheximide treatment, and the cell lysates were prepared. Western blot analysis was then used to determine the amount of proteins at various time points with specific antibodies.

The stability of protein was also determined by pulse-chase analysis. Approximately  $1 \times 10^6$  transfected human 293T cells were incubated in methionine- and cysteine-free DMEM (Gibco BRL) for 40 min at 24 h posttransfection. Medium was then removed and replaced with fresh methionine-free DMEM containing 200  $\mu$ Ci/ml EXPRE<sup>35S</sup> protein labeling mix (PerkinElmer Life Sciences). Cells were labeled for 30 min at 37°C and washed twice with DMEM, and complete DMEM with 10% FBS was added. Cells were harvested at various time points and lysed in 500  $\mu$ l ice-cold IP buffer for 1 h. The lysates were then centrifuged at 16,000  $\times$  g for 15 min, and equal counts per minute of the lysates were immunoprecipitated with specific antibody and protein G beads. The beads were washed four times with IP buffer, suspended in sample buffer, and then separated by SDS-PAGE. The gel was then analyzed by fluorography and exposed to film overnight. The band intensities were quantitated with NIH Image software.

**Nucleotide sequence accession number.** The GenBank accession number for the KSHV sequences reported in this study is KSU75698.

## RESULTS

**K-RBP exhibits transcriptional repression activity in an HDAC-independent manner.** We previously identified a KSHV-RTA binding protein named K-RBP by yeast two-hybrid screening using a B-cell cDNA library (80). K-RBP is a novel cellular protein generated from a multiply spliced message derived from the human chromosome 19 clone CTC-543D15 (GenBank accession number AC008567), and the normal cellular function of K-RBP is unknown. K-RBP contains a KRAB domain and multiple C<sub>2</sub>H<sub>2</sub> zinc finger motifs, including one nontypical C<sub>2</sub>H<sub>2</sub> zinc finger and 11 typical C<sub>2</sub>H<sub>2</sub> zinc fingers, suggesting that it belongs to the KRAB-containing zinc finger protein family (Fig. 1A). Since most members of this protein family have been shown to function as transcriptional repressors through their KRAB domains and bind DNA via their zinc finger motifs (14, 57, 75, 87), we anticipated that K-RBP functions as a transcriptional repressor and mediates repression through its KRAB domain.

To investigate whether K-RBP possesses transcriptional repression function we used the GAL4BD fusion protein-GAL4-luciferase reporter system, since the potential DNA-binding sequence of K-RBP zinc finger motifs is unknown. This system relies on GAL4BD fusion protein binding to the GAL4 binding element in the promoter regulatory region of luciferase reporter vector pFR-Luc, which contains five copies of GAL4 binding element (Fig. 1B) and has been used for the analysis of transcription factors in mammalian cells (51, 60, 86). We generated pBDK-RBP, a full-length GAL4BD and K-RBP fusion protein expression construct, and cotransfected it with pFR-Luc. The presence of pBDK-RBP was found to strongly repress the luciferase reporter activity at a level higher than the repression induced by the well-characterized KOX1 KRAB domain that was used as a positive control (Fig. 1C) (40, 49). As expected, the K-RBP construct pcDNAK-RBP did not repress the luciferase reporter gene expression, since it is unlikely that K-RBP itself will bind to the GAL4 elements of pFR-luc in the absence of GAL4BD. The expression of each construct was verified by Western blotting using the specific antibodies (Fig. 1D). These data suggest that K-RBP functions as a transcriptional repressor when tethered to the target promoter.

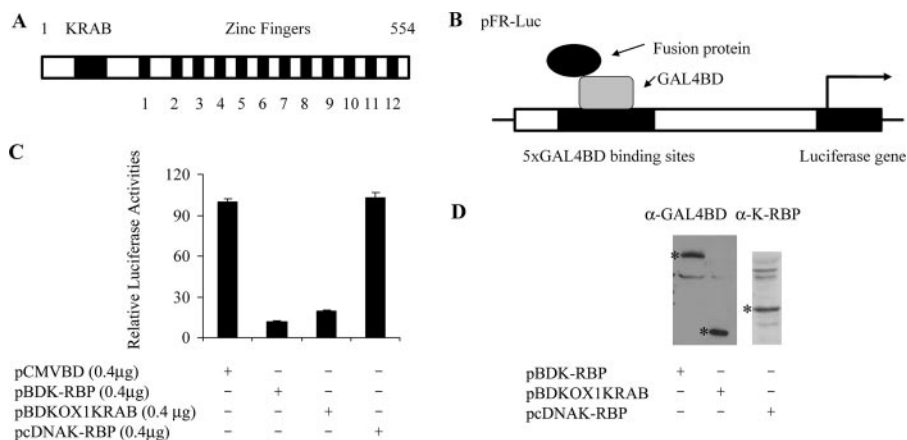


FIG. 1. K-RBP is a transcriptional repressor. (A) Schematic representation of K-RBP, including a putative KRAB domain and 12 zinc finger motifs. (B) The GAL4BD fusion protein-GAL4-luciferase reporter system. (C) K-RBP exhibits transcriptional repression activity when it is tethered to the promoter region of reporter plasmid. The expression plasmids pcDNAK-RBP, pBDK-RBP, and pBDKOX1KRAB were transfected into 293T cells along with the reporter plasmid pFR-Luc (0.25 μg). Error bars indicate standard deviations. The luciferase activity with control plasmid was normalized to 100. (D) The proteins expressed by the plasmids used as described for panel C were detected by Western blot analysis using the indicated antibodies. Asterisks indicate the specific proteins detected.

To determine whether the KRAB domain of K-RBP mediates the repression, we analyzed the putative KRAB domain from aa 42 to 98 and aligned it with several other KRAB domains by use of the alignment program of Vector NTI suite 8 (Invitrogen) to determine its similarity to the KRAB domains of other transcriptional repressors. The KRAB domains of ZNF40, ZNF133, ZNF140, KOX1, KID-1, ZBRK1, RBAK1, Hkr18, and Hkr19 (GenBank accession numbers P15822, AAH01887, AAH40561, AAH24182, AAH47105, AAG17439, AAF43389, Q9HCG1, and Q96JC4, respectively) were used in this comparison (Fig. 2A). These domains contain KRAB A and B boxes (37), and the alignment showed that K-RBP KRAB domain contains almost all the conserved amino acids in the KRAB domain (Fig. 2A) (2), indicating that the KRAB domain of K-RBP belongs to the KRAB AB subfamily. Since all the KRAB domains identified have been shown to repress transcription (75), it is likely that KRBP KRAB domain is responsible for the suppressive function of K-RBP.

To verify that the KRAB domain of K-RBP is responsible for the repression function of K-RBP, several GAL4BD and K-RBP deletion fusion proteins were generated. Both pBDK-RBP1-213 and pBDK-RBP42-98 express the KRAB domain. Clone pBDK-RBP99-554 expresses the 12 zinc finger motifs but lacks the KRAB domain, and clone pBDK-RBP99-213 expresses the domain that contain only the nontypical C<sub>2</sub>H<sub>2</sub> zinc finger motif (Fig. 2B). As shown in Fig. 2C, the presence of pBDK-RBP1-213, pBDK-RBP42-98, or pBDK-RBP repressed the luciferase reporter gene expression, while the presence of pBDK-RBP99-554 and pBDK-RBP99-213 did not. The presence of pBDK-RBP99-213 was found to activate transcription four- to fivefold. The full-length K-RBP construct pBDK-RBP exhibited the strongest activity and repressed transcription by more than 90%, while the KRAB construct pBDK-RBP42-98 expressing the domain (42 to 98 aa) alone exhibited the weakest activity and repressed transcription by about 50% (Fig. 2C). The repression by K-RBP and the KRAB domain (K-RBP42-98) was found to be dose dependent (Fig.

2E and F). These data suggest that the KRAB domain is responsible for the repression function of K-RBP but that optimal repression requires a region other than the KRAB domain of K-RBP. The inability of some of the constructs to repress was not due to defects at the protein expression level, since the presence of all the GAL4BD-fused K-RBP deletion proteins was verified by Western blotting (Fig. 2D).

The repression function of some KRAB-containing zinc finger proteins was shown to involve HDACs which remove the acetyl groups that silence transcription (64), whereas others, such as KOX1, mediate repression through an HDAC-independent mechanism (40). We found that HDACs have little effect on the repression function of K-RBP, because the addition of trichostatin A, a potent inhibitor of HDACs, has little effect on the K-RBP repression activity (Fig. 3A). In addition, the overexpression of CBP and p300 encoded by pHACBP and pCMVβp300, which possess histone acetyltransferase activities and are antagonists for HDACs (53), did not relieve the K-RBP-mediated repression of the reporter gene expression (Fig. 3B). In contrast, the presence of CBP and p300 expression enhances K-RBP-mediated repression (Fig. 3B). This may be due to overexpression of CBP and p300 altering the cellular environment and leading to more K-RBP protein being expressed. This was in fact the case, as demonstrated by the results of Western blot analysis (Fig. 3C). Taken together, the results described above suggest that K-RBP-mediated repression is HDAC independent.

**K-RBP interacts with TIF1β, a corepressor of KRAB-containing zinc finger proteins.** The KRAB domains from several KRAB-containing zinc finger proteins have been shown to physically interact with TIF1β, a transcriptional corepressor for KRAB-containing proteins (1, 2, 26, 31, 47, 48). Since K-RBP is a KRAB-containing transcriptional repressor and contains the crucial amino acids (DV and MLE) needed for TIF1β interaction (Fig. 2A) (12), we then examined whether K-RBP also associates with TIF1β by use of the yeast two-

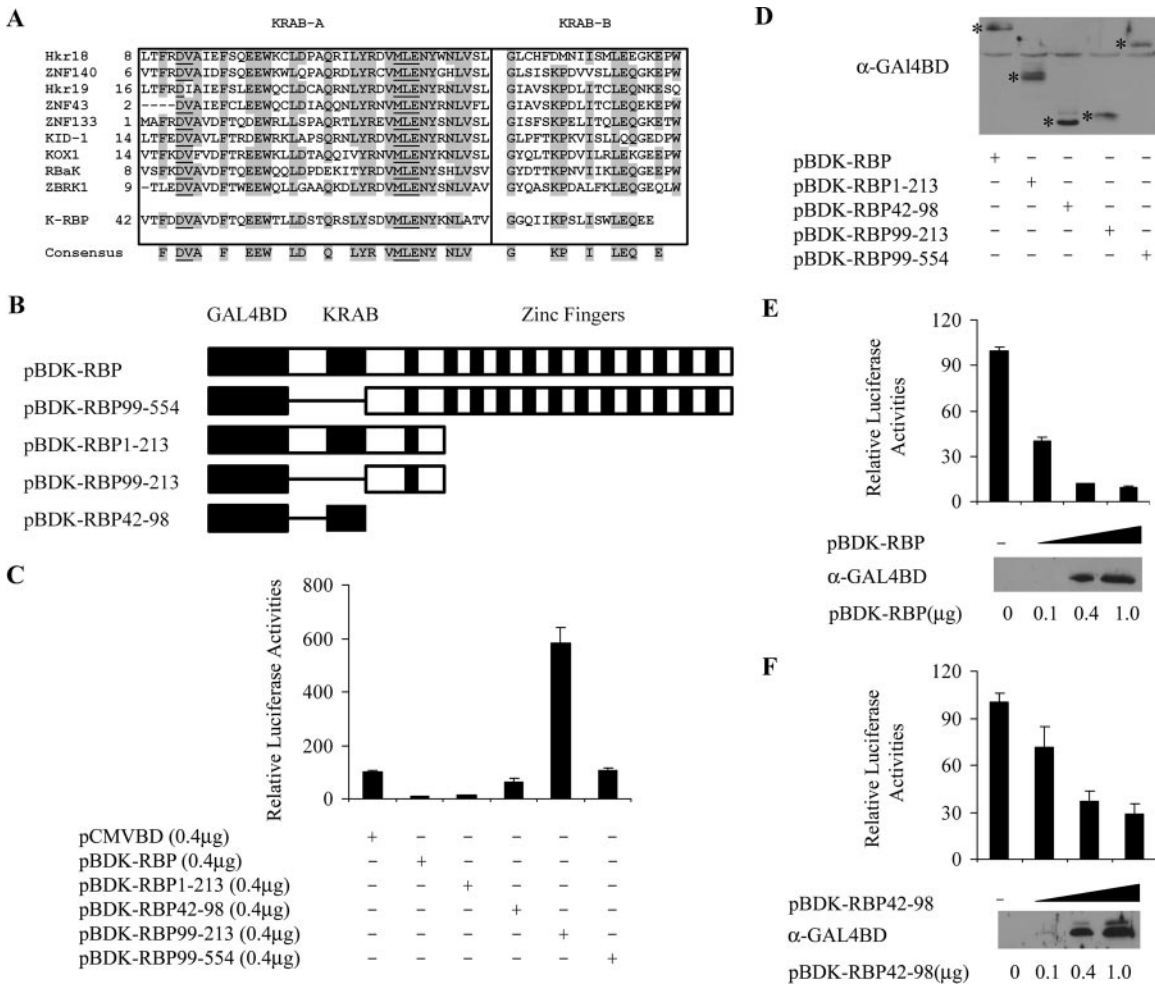


FIG. 2. Transcriptional repression activity of K-RBP. (A) Comparison of putative K-RBP KRAB domain with KRAB domains from other KRAB-containing zinc finger proteins (ZNF40, ZNF133, ZNF140, KOX1, KID-1, ZBRK1, RBaK1, Hkr18, and Hkr19; GenBank accession numbers P15822, AAH01887, AAH40561, AAH24182, AAH47105, AAG17439, AAF43389, Q9HCG1, and Q96JC4, respectively). KRAB-A and KRAB-B boxes are indicated. Dashes (-) show gaps among the aligned sequences. Conserved amino acids of KRAB domain are shaded, and a consensus sequence is shown at the bottom. The crucial amino acids for TIF1 $\beta$  interaction are underlined. Alignment was performed using Vector NTI suite 8 (Invitrogen). (B) Schematic diagram of K-RBP deletion mutants used to determine the domain responsible for the repression activity of K-RBP. (C) Transcriptional activity of K-RBP mutants. Different GAL4BDK-RBP mutant constructs were cotransfected with the reporter plasmid pFR-luc (0.25  $\mu$ g) into 293T cells, and luciferase activities were measured at 24 h after transfection. Error bars indicate standard deviations. The luciferase activity with control plasmid was normalized to 100. (D) Western blot analysis using antibody against GAL4BD with lysates of cells transfected with different K-RBP mutants to determine the expression of the K-RBP mutant proteins. Asterisks indicate the specific proteins detected. (E) The repression activity of K-RBP is dose dependent. Various amounts of pBDK-RBP expression plasmid were cotransfected with reporter plasmid pFR-luc (0.25  $\mu$ g) into 293T cells. The results of Western blot analysis of the expression of GAL4BDK-RBP by use of antibody against GAL4BD are shown at the bottom. Error bars indicate standard deviations. The luciferase activity with control plasmid was normalized to 100. (F) The repression activity of KRAB domain is dose dependent. Experiments were carried out as described for panel E, except pBDK-RBP42-98 plasmid was used.

hybrid assay. As shown in Table 1, cotransformation of plasmids pGBKK-RBP, which expresses GAL4BD-fused K-RBP, and pGADTIF1 $\beta$ , which expresses GAL4AD-fused TIF1 $\beta$ , activated the expression of reporter genes. The K-RBP domain that is responsible for the interaction with TIF1 $\beta$  was mapped to its first 213 aa, a region which contains its KRAB domain, since clone pGBKK-RBP214-554, which expresses the zinc finger domain of K-RBP, was not active when cotransformed with pGADTIF1 $\beta$ . However, we could not demonstrate the interaction between K-RBP1-213 and TIF1 $\beta$  directly by yeast two-hybrid analysis, since clones pGBKK-RBP1-213, which expresses

the first 213 aa, and pGBKK-RBP42-98, which expresses the KRAB domain, were found to activate the reporter gene by themselves. The domain consisting of the first 423 aa of TIF1 $\beta$  (clone pGADTIF1 $\beta$ 1-423), which has previously been shown to interact with other KRAB domains, can interact with K-RBP (48) (Table 1). No activation was observed with either pGADTIF1 $\beta$  or pGBKK-RBP cotransformed with the control plasmids (pGBKT7 or pGADT7).

The interaction between K-RBP and TIF1 $\beta$  was further confirmed by coimmunoprecipitation in 293T cells. Flag-tagged TIF1 $\beta$  protein encoded by pCMVTIF1 $\beta$ Flag could be coim-

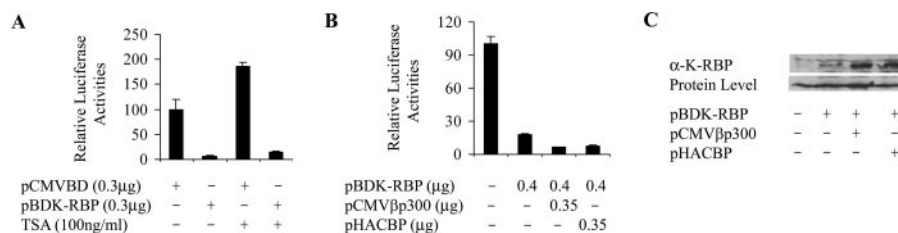


FIG. 3. The repression activity of K-RBP is HDAC independent. (A) The effect of HDAC inhibition on transcriptional repression activity of K-RBP. 293T cells were transfected with the indicated plasmids and pFR-luc (0.25 μg). At 14 h posttransfection, the cells were treated with trichostatin A (TSA) or vehicle control (dimethyl sulfoxide) for another 20 h and then lysed, and luciferase activities were measured. (B) Effect of overexpression of pCMVβp300 or pHACBP on the repression activity of K-RBP. 293T cells were transfected with indicated plasmids along with pFR-luc (0.25 μg). Luciferase activities were measured at 24 h after transfection. Error bars indicate standard deviations. The luciferase activity with control plasmid pCMVBD was normalized to 100. (C) Western blot analysis of cell lysates prepared from the transfected cells as described for panel B to detect the expression of pBDK-RBP by use of antibody against K-RBP.

munoprecipitated with HA-tagged K-RBP protein encoded by pHAK-RBP in the presence of anti-HA antibody but not with pCMVHA, which only expresses the HA tag (Fig. 4A). Moreover, Flag-tagged TIF1β protein could be coimmunoprecipitated by an HA-tagged K-RBP1-213 containing the KRAB domain, whereas an HA-tagged construct pHAK-RBP214-554 containing the K-RBP zinc finger motifs failed to coimmunoprecipitate TIF1β (Fig. 4A). This finding is consistent with the yeast two-hybrid results and indicates that the KRAB domain mediates the interaction between K-RBP and TIF1β. Similarly, coimmunoprecipitation also demonstrated that HA-tagged K-RBP and HA-tagged K-RBP1-213 could be coimmunoprecipitated with Flag-tagged TIF1β protein in the presence of anti-Flag antibody (Fig. 4B). Furthermore, endogenous K-RBP protein was shown to interact with HA-tagged TIF1β by using anti-K-RBP antibody to immunoprecipitate K-RBP in 293T cells transfected with pHATIF1β. The HA-tagged TIF1β protein was detected by Western blot analysis using anti-HA antibody as a probe after anti-K-RBP precipitation. The pre-immune serum for K-RBP did not precipitate the HATIF1β (Fig. 4C). Taken together, these results demonstrate that K-RBP can bind to the corepressor TIF1β, using it as a corepres-

sor, in similarity to what was observed with other KRAB-containing zinc finger proteins.

**TIF1β stabilizes K-RBP.** During the analysis of K-RBP, a much higher level of K-RBP protein in the presence of overexpressed TIF1β was observed (Fig. 5A, left panel), but the level of K-RBP mRNA remained unchanged, as determined by semiquantitative RT-PCR (Fig. 5A, right panel). The results described above suggest that TIF1β may stabilize K-RBP and extend its half-life. To confirm this observation, we examined the temporal levels of K-RBP in 293T cells which were co-transfected with pHAK-RBP and pCMVTIF1βFlag in the presence of cycloheximide treatment to prevent new protein synthesis. The K-RBP expression was determined by Western blot analysis using anti-K-RBP antibody (Fig. 5B). γ-Tubulin, which has a long half-life, was used as a control. The stability of K-RBP was found to be enhanced in the presence of overexpressed TIF1β. In the absence of TIF1β, K-RBP protein could not be detected at 90 min after cycloheximide treatment, whereas in the presence of TIF1β, K-RBP protein could still be detected at 450 min. This result was further confirmed by pulse-chase analysis using 293T cells transfected with pHAK-RBP either with or without pCMVTIF1βFlag. As shown in Fig. 5C, K-RBP has a much longer half-life when coexpressed with TIF1β. The half-life of K-RBP was approximately 30 min in the absence of TIF1β, while its half-life was estimated to be up to 150 min in the presence of TIF1β. Our results thus support the notion that TIF1β extends the half-life of K-RBP.

We next sought to test whether the interaction between TIF1β and K-RBP is sufficient for K-RBP stabilization by use of various TIF1β mutants (Fig. 5D). The TIF1β mutant pHATIF1β1-423, which retains the interaction domain with K-RBP, failed to stabilize K-RBP. The TIF1β mutant pHATIF1β442-835, which does not interact with K-RBP, also failed to stabilize K-RBP. Our result suggests that the interaction between K-RBP and TIF1β alone is not sufficient to protect K-RBP from degradation.

**K-RBP modulates RTA-mediated transcriptional activation of several KSHV promoters.** Since K-RBP was first identified via its interaction with RTA, we tested the effect of K-RBP on RTA-induced transactivation of several viral promoters in 293T cells. As observed earlier (80), K-RBP was found to enhance RTA-mediated transactivation of ORF8 (pK8Pluc) and ORF57 (p57Pluc1) promoters when

TABLE 1. Reporter gene expression by yeast (AH109) transformants<sup>a</sup>

Plasmid with GAL4BD	Plasmid with GAL4AD	LacZ expression <sup>b</sup>	His/Ade expression <sup>c</sup>
pGBKK-RBP	pGADTIF1β	+	+
pGBKK-RBP	pGADTIF1β1-423	++	++
pGBKK-RBP	pGADTIF1β442-835	-	-
pGBKK-RBP214-554	pGADTIF1β	-	-
pGBKT7	pGADTIF1β	-	-
pGBKT7	pGADTIF1β1-423	-	-
pGBKT7	pGADTIF1β442-835	-	-
pGBKK-RBP	pGADT7	-	-
pGBKK-RBP214-554	pGADT7	-	-
pGBKK-RBP1-213	pGADT7	++	+
pGBKK-RBP42-98	pGADT7	++	+

<sup>a</sup> AH109 was cotransformed with the indicated GAL4BD and GAL4AD plasmids. Cotransformants were selected using nutrition selection markers for the vectors. The phenotypes of the colonies were analyzed by filter β-Gal assays and by their growth on synthetic dropout medium (SD) plates lacking His and Ade.

<sup>b</sup> ++, intense blue color development within 3 h in the filter paper β-Gal assays; +, intense blue color development within 6 h in the filter paper β-Gal assays; -, clone was unable to develop color in 8 h.

<sup>c</sup> ++, colonies appeared after 2 days of incubation at 30°C on SD plates lacking His and Ade; +, colonies appeared after 3 days; -, no growth.

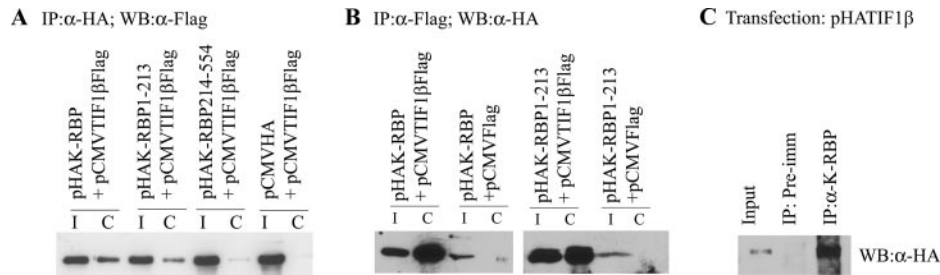


FIG. 4. Coimmunoprecipitation assays to demonstrate the interaction between K-RBP and corepressor TIF1 $\beta$ . (A) TIF1 $\beta$  can be coimmunoprecipitated with K-RBP. Lysates prepared from 293T cells transfected with the indicated plasmids were subjected to immunoprecipitation with an anti-HA antibody followed by anti-Flag immunoblotting. (B) K-RBP and K-RBP1-213 coimmunoprecipitated with TIF1 $\beta$ . Lysates prepared from 293T cells transfected with the indicated plasmids were subjected to immunoprecipitation with an anti-Flag antibody followed by anti-HA immunoblotting. (C) Endogenous K-RBP interacts with TIF1 $\beta$ . Lysate from 293T cells transfected with pHATIF1 $\beta$  plasmid was subjected to immunoprecipitation using anti-K-RBP antibody or preimmune serum followed by immunoblotting with anti-HA antibody. I represents input, C represents coimmunoprecipitation. WB, Western blotting.

expressed at low concentrations (Fig. 6 A and B) (80). However, K-RBP was found to inhibit RTA-mediated transactivation of KSHV ORFK8 and ORF57 promoters when increasing amounts of K-RBP expression plasmid were added (Fig. 6A and B). More than 50% inhibition was observed when the highest amount of K-RBP was tested. The repression was also observed with the KSHV PAN promoter (pPANpluc), and K-RBP suppressed RTA-mediated PAN

promoter activation by 30% (Fig. 6C). The repression is not due to an effect on RTA expression, because K-RBP was found to have no effect on RTA expression level, as determined by Western blot analysis (Fig. 6D). We also tested whether K-RBP can suppress RTA-mediated transactivation in Vero cells and found that overexpression of K-RBP can indeed repress RTA-mediated transactivation of PAN (Fig. 6E), ORF57, and K8 promoters (data not shown).

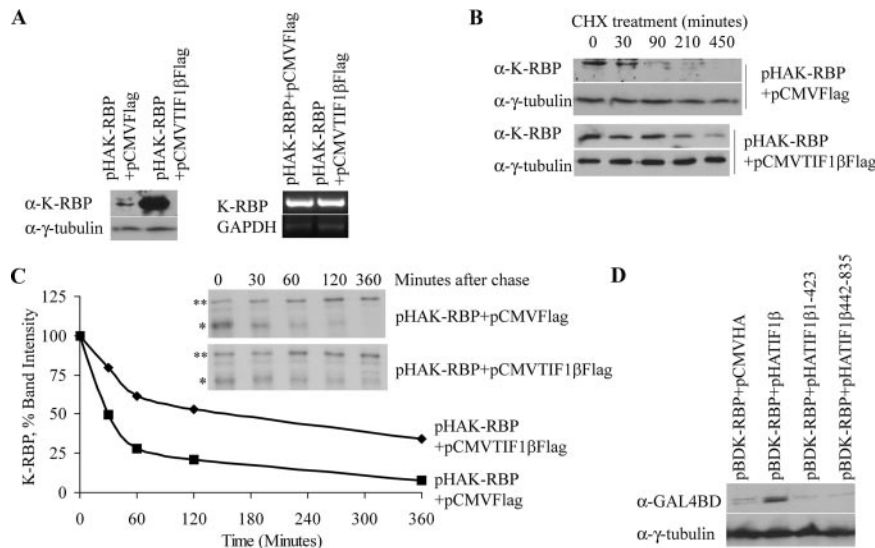


FIG. 5. TIF1 $\beta$  stabilizes K-RBP. (A) Left panel, Western blot analysis of K-RBP in lysates made from 293T cells transfected with pHAK-RBP in the presence or absence of pCMVTIF1 $\beta$ Flag. Equivalent amounts of proteins were loaded in each lane, as confirmed by Western blot analysis using  $\gamma$ -tubulin as a control. Right panel, RT-PCR analysis of K-RBP RNA expression isolated from transfected cells represented in the left panel. Equivalent amounts of RNA were used in RT-PCR for each experiment, as confirmed by RT-PCR employing the GAPDH gene, which was used as an internal control. (B) The effect of TIF1 $\beta$  on K-RBP upon cycloheximide (CHX) treatment. The 293T cells transfected with pHAK-RBP in the presence of control plasmid or pCMVTIF1 $\beta$ Flag were harvested at different time points after pretreatment with 75  $\mu$ g/ml cycloheximide and analyzed by Western blotting. The K-RBP expression levels were analyzed with anti-K-RBP antibody.  $\gamma$ -Tubulin was used as an internal control. (C) The effect of TIF1 $\beta$  on the stability of K-RBP, as measured by pulse-chase analysis. The results of pulse-chase analysis of [ $^{35}$ S]methionine-radiolabeled 293T cells transfected with pHAK-RBP in the presence of control plasmid or pCMVTIF1 $\beta$ Flag are presented. Cells were radiolabeled with 200  $\mu$ Ci/ml [ $^{35}$ S]methionine for 30 min and chased for the indicated times with unlabeled methionine. Lysates were immunoprecipitated with polyclonal anti-HA antibody. The graph depicts densitometric analysis of a representative experiment, the results of which indicate that K-RBP has an estimated half-life of 30 min in the absence of TIF1 $\beta$  and of 150 min in the presence of TIF1 $\beta$ . The K-RBP bands were expressed as percentages of intensities, with band intensity at time 0 equal to 100%. The single asterisks indicate K-RBP protein, while the double asterisks indicate a nonspecific cellular protein band which was used as the internal loading control. (D) Western blot analysis of GAL4BDK-RBP in lysates of 293T cells transfected with pBDK-RBP in the presence of pCMVHA, pHATIF1 $\beta$ , pHATIF1 $\beta$ 1-423, or pHATIF1 $\beta$ 442-835. Equivalent amounts of proteins were loaded in each lane, as confirmed by Western blot analysis using  $\gamma$ -tubulin as an internal control.

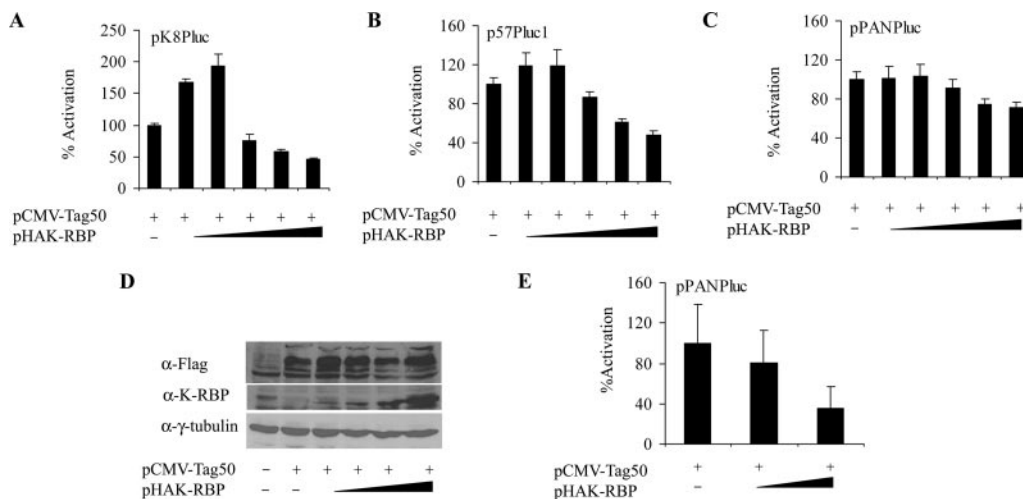


FIG. 6. K-RBP can downregulate RTA-mediated transcriptional activation of KSHV promoters. (A) 293T cells were transfected with the reporter construct pK8Pluc (7.5 ng), a fixed amount (25 ng) of pCMV-Tag50, and increasing amounts (0, 10, 25, 75, 750, and 1,500 ng) of pHAK-RBP. Luciferase activities were measured at 24 h after transfection. Luciferase reporter activities are expressed as a percentage of activation, with activation by RTA alone equal to 100%. The error bars indicate standard deviations. (B) Transfection was carried out as described for panel A, except reporter construct p57Pluc1 (20 ng) was used. (C) Transfection was carried out as described for panel A, except reporter construct pPANPluc (20 ng) was used. (D) Western blot analysis of RTA expression in the presence of increasing amounts of K-RBP expression. Lysates of 293T cells transfected with same amount of pCMV-Tag50 and increasing amounts of pHAK-RBP were used in the immunoblotting using anti-Flag and anti-K-RBP antibodies. The  $\gamma$ -tubulin level was used to indicate that comparable amounts of each sample were loaded in each lane. (E) Vero cells were transfected with reporter construct pPANPluc (50 ng), a fixed amount (50 ng) of pCMV-Tag50, and increasing amounts (0, 100, and 250 ng) of pHAK-RBP. Luciferase activities were measured at 48 h after transfection. Luciferase reporter activities are expressed as a percentage of activation.

**TIF1 $\beta$  participates in the repression of RTA-mediated transactivation of KSHV promoters.** Both TIF1 $\beta$  and RTA interact with K-RBP, and TIF1 $\beta$  is a potential corepressor of K-RBP; therefore, we hypothesized that TIF1 $\beta$  may also be involved in regulating RTA-mediated transactivation, possibly indirectly via its interaction with K-RBP. We then examined the effect of TIF1 $\beta$  on RTA-mediated transactivation of KSHV ORFK8, ORF57, and PAN promoters. Overexpression of pHTIF1 $\beta$  repressed RTA-mediated transactivation of both ORFK8 and ORF57 promoters by about 40 to 50% (Fig. 7A, B, E, and F). No significant repression was observed with the PAN promoter (Fig. 7C), suggesting a promoter-dependent effect. In similarity to K-RBP, TIF1 $\beta$  had no effect on the RTA protein expression (Fig. 7D). Overexpression of both TIF1 $\beta$  and K-RBP led to a synergistic effect on the RTA-mediated transactivation of K8 and ORF57 promoters, with 50 to 70% repression (Fig. 7E and F). This is reflected at the protein level; the presence of TIF1 $\beta$  led to an increase of K-RBP protein (Fig. 7G). The presence of TIF1 $\beta$  also led to a slight enhancement of RTA, but the increase was not observed consistently. Our results nevertheless suggest that TIF1 $\beta$  and K-RBP synergize in the suppression of RTA-mediated transactivation. TIF1 $\beta$  may be recruited to the promoter by K-RBP, which then stabilizes K-RBP to enhance its repression of RTA-mediated transactivation. We also tested whether knockdown of endogenous K-RBP and TIF1 $\beta$  can lead to an enhancement of RTA-mediated transactivation of the ORF57 promoter. The presence of K-RBP-specific siRNA but not control siRNA can enhance RTA-mediated transactivation, but the effect is only moderate (Fig. 8A). This suggests that K-RBP is only one of the many endogenous cellular factors that can suppress RTA-

mediated transactivation. Interestingly, knockdown of TIF1 $\beta$  can enhance RTA-mediated transactivation to a level higher than that of K-RBP knockdown (Fig. 8A). TIF1 $\beta$  knockdown in this experiment did not alter K-RBP expression level (Fig. 8B), suggesting that endogenous TIF1 $\beta$  may also modulate RTA-mediated transactivation of the ORF57 promoter independently of K-RBP. Knockdown of both K-RBP and TIF1 $\beta$  can enhance RTA-mediated transactivation to a level higher than the knockdown of either K-RBP or TIF1 $\beta$  alone.

**K-RBP regulates RTA-mediated KSHV reactivation from latency.** The regulation of RTA transactivation by K-RBP on viral promoters suggests that K-RBP may play a role in KSHV reactivation. To investigate the effect of K-RBP on KSHV lytic replication, we used the TReXBCBL-1 RTA cell line (50). In this cell line, the RTA gene is integrated into the BCBL-1 genome and RTA expression can be induced by tetracycline (or doxycycline). The cells were transfected with either control plasmid pcDNA3.1 (Fig. 9A, lane 1) or K-RBP expression plasmid pcDNAK-RBP (Fig. 9A, lane 2) to overexpress K-RBP. Interestingly, the expression of the early lytic gene K8 and late lytic gene K8.1 was lower in cells that were overexpressing K-RBP. Their expression was reduced by about 30 to 50%, whereas the latent gene LANA was not affected (Fig. 9A). The doxycycline-induced His-tagged RTA protein can be detected by anti-His antibody, and the total RTA from doxycycline-induced cells can be detected with anti-RTA antibody (50). K-RBP was detected in both control cells (Fig. 9A, lane 1) and K-RBP expression plasmid-transfected cells (Fig. 9A, lane 2). His-tagged RTA and total RTA levels were found to be comparable in both pcDNAK-RBP- and pcDNA3.1-transfected cells upon treatment with doxycycline (Fig. 9A). Cells

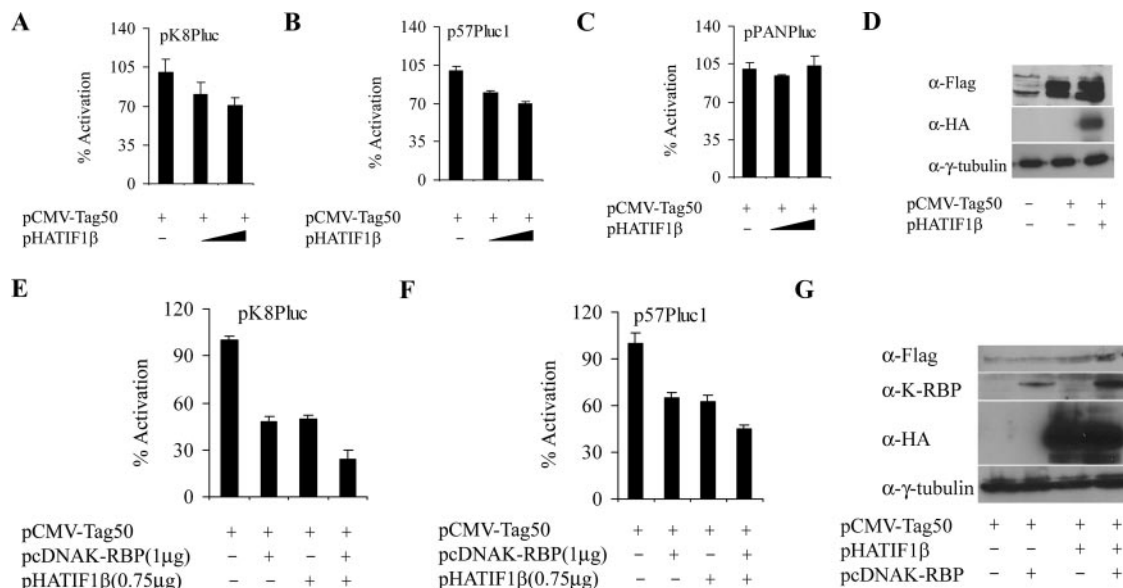


FIG. 7. TIF1 $\beta$  is involved in the downregulation of RTA-mediated transactivation of KSHV promoters. (A) 293T cells were transfected with the reporter construct pK8Pluc (7.5 ng), a fixed amount (25 ng) of pCMV-Tag50, and increasing amounts (0, 250, 750 ng) of pHATIF1 $\beta$ . Luciferase activities were measured at 24 h after transfection. Luciferase reporter activities are expressed as a percentage of activation, with activation by RTA alone equal to 100%. The error bars indicate standard deviations. (B) Transfection was carried out as described for panel A, except reporter construct p57Pluc1 (20 ng) was used. (C) Transfection was carried out as described for panel A, except reporter construct pPANPluc (20 ng) was used. (D) Western blot analysis for pCMV-Tag50 expression in transfected 293T cells in the presence or absence of pHATIF1 $\beta$ . Lysates of cells either transfected with pCMV-Tag50 alone or cotransfected with pHATIF1 $\beta$  expression plasmid were analyzed using anti-Flag, anti-HA, or anti- $\gamma$ -tubulin antibodies. (E) 293T cells were transfected with the reporter construct pK8Pluc (7.5 ng), a fixed amount (25 ng) of pCMV-Tag50, and indicated amounts of pHATIF1 $\beta$  or pcDNAK-RBP. Luciferase activities were measured at 24 h after transfection. Luciferase reporter activities are expressed as a percentage of activation, with activation by RTA alone equal to 100%. The error bars indicate standard deviations. (F) Transfection was carried out as described for panel E, except reporter construct p57Pluc1 (20 ng) was used. (G) Western blot analysis of pCMV-Tag50 expression in transfected 293T cells in the presence of pHATIF1 $\beta$ , pcDNAK-RBP, or both. Lysates of cells either transfected with pCMV-Tag50 alone or cotransfected with pHATIF1 $\beta$ , pcDNAK-RBP, or both expression plasmids were analyzed using anti-Flag, anti-HA, anti-K-RBP, or anti- $\gamma$ -tubulin antibodies.

transfected with K-RBP expression plasmid showed an enhanced level of K-RBP, but the enhancement was not substantial. This could be due to the instability of K-RBP and the difficulty in obtaining more than 50% transfection efficiency in this TReXBCBL-1 RTA cell line. The level expressed in the control results represents the normal level of K-RBP. Nevertheless, these results suggest that viral reactivation and the expression of the lytic viral gene were repressed in the presence of overexpressed K-RBP.

To further confirm the role of K-RBP in RTA-mediated KSHV reactivation, siRNA was used to knock down endogenous K-RBP expression in KSHV-infected cells to determine its effect on viral reactivation. This was carried out by using Vero cells that were infected by a recombinant green fluorescent protein-red fluorescent protein (GFP-RFP) double-labeled rKSHV.219 virus (76). In this cell line, KSHV latently infected cells constitutively express GFP. Upon induction by RTA, cells that are lytically reactivated express RFP under the control of the lytic PAN promoter and can be quantitated. When the expression of K-RBP was knocked down by siRNA (Fig. 9B), the number of cells harboring reactivated KSHV was higher upon induction by RTA compared to the number of cells that were transfected with a control siRNA (Fig. 9C). Two to three times more cells containing reactivated viruses were consistently observed when KSHV lytic replication was induced by expressing RTA in K-RBP knockdown cells (Fig.

9D). The enhancement was confirmed by measuring the amount of viruses released in supernatant. The amount of viral DNA was measured by PCR amplification of the ORF26 of KSHV (Fig. 9E and F). Real-time PCR consistently detected a two-fold-higher viral DNA level in medium of cells transfected with K-RBP siRNA (Fig. 9F). In summary, these results suggest that K-RBP can suppress KSHV lytic reactivation and that this suppression may be in part mediated by the repression of K-RBP in RTA-mediated transactivation of lytic gene expression.

## DISCUSSION

It is estimated that there are more than 300 members of KRAB-containing zinc finger proteins encoded in the human genome (58), and some of them have been shown to function as transcriptional repressors and play a role in gene silencing. They have also been shown to have diverse functions, including the maintenance of nucleus, cell differentiation, cell proliferation, apoptosis, and neoplastic transformation (13, 20, 24, 25, 71, 74, 83). These functions can be mediated directly or indirectly by DNA binding activity of the zinc finger motifs within these proteins or mediated by protein-protein interactions between KRAB-containing zinc finger proteins and other proteins. TIF1 $\beta$  has been suggested to function as a molecule targeted to promoter elements via its interaction with KRAB-

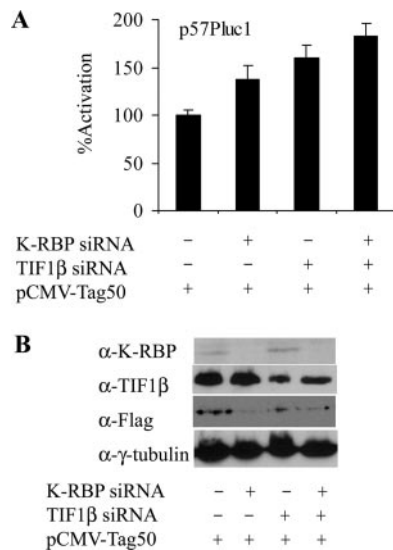


FIG. 8. Knockdown of K-RBP and TIF1β enhances RTA-mediated transactivation of the ORF57 promoter. (A) 293T cells were transfected with indicated siRNA. The total amount of siRNA in each well was normalized by use of the control siRNA. At 24 h after siRNA transfection, the reporter construct p57Pluc1 (20 ng) and RTA expression plasmid pCMV-Tag50 (25 ng) were transfected into the cells. Luciferase activities were measured at 24 h after transfection. Luciferase reporter activities were expressed as a percentage of activation, with activation by RTA with control siRNA made equal to 100%. The error bars indicate standard deviations. (B) Western blot analysis of the expression of RTA, TIF1β, K-RBP, and tubulin in cells transfected using different siRNAs, identical amounts of pCMV-Tag50, and indicated antibodies.

containing zinc finger proteins. The HDAC-SETDB1 methylation complex and HP1 proteins are then recruited to the promoter region and form a facultative heterochromatin environment on the target promoter (63). TIF1β was shown to play a crucial role in KRAB-mediated repression, and a mutant of the KRAB domain of KRAB-containing zinc finger proteins that cannot interact with TIF1β lost its repression function (12). TIF1β interacts and synergizes with K-RBP to repress RTA-mediated transactivation, suggesting that TIF1β serves as a corepressor of K-RBP in similarity to the results seen with other KRAB-containing zinc finger proteins. The stabilization of K-RBP by TIF1β suggests that TIF1β not only functions as a molecular scaffold for K-RBP to mediate repression but also protects K-RBP from degradation to function as a transcriptional repressor. Two other KRAB-containing proteins, c-Myc-interacting Krim-1 and Krim-2, were also found to be stabilized by TIF1β (20).

We could not rule out the possibility that K-RBP also regulates RTA transactivation through a KRAB domain-independent mechanism, since there are several possible mechanisms for K-RBP to regulate RTA function. First, K-RBP may bind directly to DNA elements in the KSHV promoters to mediate repression. This is consistent with the notion that zinc finger motifs are DNA binding modules, and several KRAB-containing zinc finger proteins were found to have site-specific DNA binding activity. We are currently in the process of carrying out experiments to examine the potential DNA binding activity of K-RBP and to determine whether such binding is necessary for

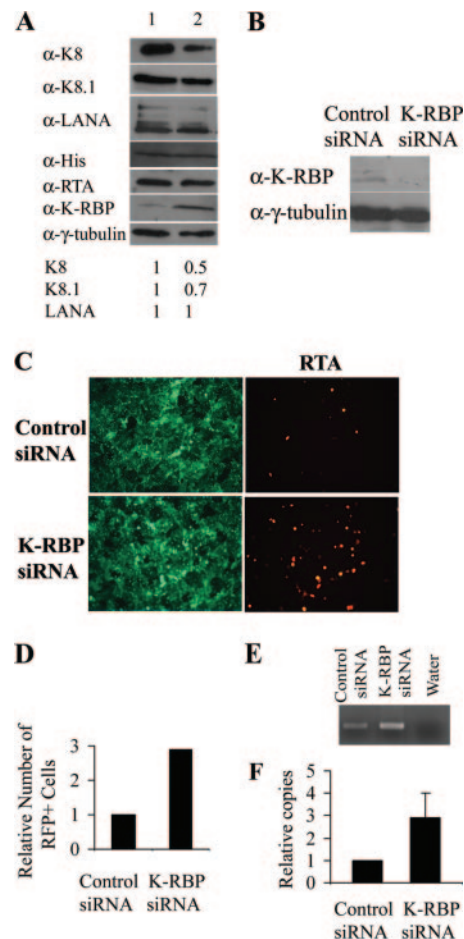


FIG. 9. K-RBP represses RTA-mediated KSHV lytic replication. (A) TRExBCBL-1RTA cells were transfected either with pCDNA3.1 (lane 1) or with pCDNAK-RBP (lane 2). At 24 h posttransfection, cells were treated with 1 μg/ml doxycycline to induce lytic replication of KSHV. At 6 h (His-tagged RTA, RTA, and K8) and 24 h (K8.1 and LANA) posttransfection, cells were harvested, lysed, and separated by SDS-PAGE, and Western blot analysis was performed using antibodies as indicated. Numbers indicate the relative amounts of K8, K8.1, and LANA proteins. (B) Vero cells harboring rKSHV.219 were transfected with control or K-RBP siRNA to knock down K-RBP expression, and K-RBP protein was analyzed by Western blotting using anti-K-RBP antibody. (C) KSHV-infected cells were infected by baculovirus expressing KSHV-RTA to induce KSHV lytic replication. At 72 h after infection, latently infected cells were detected by GFP expression and cells with lytic KSHV replication were detected by RFP expression. The cells with latent and lytic KSHV replication were observed under microscopy. (D) The numbers of cells expressing RFP as described for panel C were compared between control and K-RBP siRNA-treated cells. The number of RFP-positive cells in control siRNA-treated cells was normalized to 1. (E) KSHV-infected cells were infected by baculovirus expressing KSHV-RTA to induce KSHV lytic replication. At 96 h after infection, supernatants of transfected cells were harvested and enriched for PCR amplification of KSHV ORF26 to detect the virion production level of KSHV. (F) The relative amounts of KSHV DNA were measured by real-time PCR, with the DNA amount of control siRNA-transfected cells normalized to 1. The error bars indicate standard deviations of the results obtained with three PCR experiments.

the regulation of RTA-mediated transactivation. Second, K-RBP may function as a competitive inhibitor of RTA either through direct interaction with RTA or by inhibiting the binding of RTA to its response elements. Third, K-RBP may func-

tion as a repressor of RTA similarly to HDAC, which was found to interact with RTA to repress RTA-mediated transactivation (17). It is possible that other cellular factors such as TIF1 $\beta$  recruited by K-RBP are also involved. The presence of TIF1 $\beta$  in the promoter region may then suppress RTA-mediated transactivation through the formation of heterochromatin. TIF1 $\beta$  could enhance the repression by functioning as a corepressor in the RTA/K-RBP complex or increase the stability of K-RBP. Further experiments are required to decipher whether one or more of these mechanisms are involved.

RTA is an important immediate-early viral protein that induces KSHV lytic replication. It can activate numerous KSHV genes, including ORF57, PAN RNA, K8, TK, LANA, and itself (6, 10, 11, 29, 46, 54, 68, 69). It has been suggested that RTA can bind to elements located in the target promoters either directly or indirectly to activate transcription (41, 68). The indirect binding involves several cellular factors. For example, RBP-J $\kappa$  was demonstrated to play a critical role in RTA binding to its response element in the ORF57 promoter (32, 33). Several other cellular factors such as C/EBP $\alpha$ , CBP/p300, and the SWI/SNF complex were found to enhance RTA transactivation and viral replication (16, 17, 81). KSHV infection has been shown to lead to initial lytic replication and limited viral production, but this is quickly followed by a shutoff of viral replication leading to latency (27), suggesting that RTA activity is downregulated in this process. In addition, KSHV is latent in many KSHV-infected cells, suggesting that RTA expression and function are tightly controlled in these cells. The downregulation of RTA is likely to involve a number of viral and cellular factors, and the viral LANA and K $\beta$ ZIP proteins were shown to be involved in shutting down RTA lytic viral replication (22, 28, 35). In addition, a number of cellular factors were found to downregulate RTA transactivation. They include HDAC, IRF-7, PARP-1, hKFC, and NF- $\kappa$ B (5, 17, 19, 78). They either posttranslationally modify RTA protein or interfere with RTA binding to its response elements in the viral promoters to suppress the RTA-mediated transactivation. K-RBP, as reported in this paper, is another cellular factor that can regulate RTA transactivation. The effect of K-RBP on RTA transactivation appears to be dose dependent. In transfection assays, we have previously shown that K-RBP activated RTA-mediated transactivation (80). This was substantiated when K-RBP was expressed at low concentrations. However, with an increasing amount of K-RBP, as reported here, it acts as a repressor of transcription, in similarity to what was observed with other KRAB-containing zinc finger proteins. The various effects of K-RBP on RTA could be due to the effect of RTA and K-RBP on the expression of a number of cellular genes that can either up- or downregulate the interplay between RTA and K-RBP or could be due to different cellular factors present in the promoter regions with various amounts of K-RBP protein. These effects may lead to feedback regulation that is usually highly dosage dependent. In addition, K-RBP may play different roles in different stages of KSHV reactivation and de novo infection and in different cell types when the expression levels of RTA and K-RBP vary. Since RTA is known to complex with a number of viral and cellular proteins, including K-RBP, it is likely that the modulation of RTA function by these cellular and viral factors contributes to the regulation of KSHV lytic replication. Further studies of

how these factors and RTA interact may lead to new strategies to control the switch of KSHV to lytic replication from latency.

In our study, overexpression of K-RBP in TReXBCBL-1RTA cells suppressed KSHV lytic replication. This suggests that K-RBP could be the negative regulator in RTA-mediated KSHV reactivation. This was confirmed by K-RBP knockdown experiments using Vero cells latently infected by KSHV. The knockdown of K-RBP can enhance lytic viral reactivation. However, even though the effect of K-RBP on KSHV lytic replication is consistent, neither the overexpression of K-RBP nor its knockdown led to a dramatic effect on KSHV lytic replication. Overexpression of K-RBP led to a 30 to 50% reduction of expression of lytic proteins K8 and K8.1. Similarly, K-RBP knockdown led to a two- to threefold increase in lytic replication upon RTA induction. This is likely due to the involvement of a number of other viral and cellular proteins in the RTA-mediated regulation of lytic replication, and K-RBP is only one of a number of cellular factors involved. Many of them may have overlapping functions, so the overexpression or elimination of one, such as K-RBP, would not have an overwhelming effect on KSHV lytic replication. In addition, K-RBP could not be completely knocked out by siRNA with a low level of K-RBP still being expressed and may have an effect on viral replication. Moreover, the knockdown study was not carried out using B cells, since K-RBP could not be knocked down efficiently in the various B-cell lines that were tested. At this point, we cannot rule out the possibility that K-RBP affects KSHV reactivation indirectly through an RTA-independent pathway, but it is likely that the suppression of RTA by K-RBP contributes to the suppression of KSHV reactivation and the establishment of KSHV latency.

K-RBP is ubiquitously expressed in different cell lines and tissues (66, 80), but little is known about the normal function of this protein and its role in the regulation of RTA function. Our study thus demonstrated that this KRAB-containing zinc finger protein could function as a transcriptional repressor and that it is involved in the regulation of KSHV transcriptional activator RTA and in KSHV gene expression and reactivation. This study not only added a new member to the KRAB-containing zinc finger protein family experimentally but also added a novel function to this protein family, namely, its involvement in the regulation of KSHV viral gene expression, and has provided new insights with respect to studying the regulation of KSHV latency and lytic replication.

#### ACKNOWLEDGMENTS

This study was supported by PHS grant CA76958 and NCCR COBRE grant RR15635 to C.W.

We thank Jae Jung at Harvard Medical School, Walter Schaffner at Universität Zürich, Clinton Jones at University of Nebraska, Bala Chandran at Rosalind Franklin University, Jeffrey Viera at University of Washington, and Frank J. Rauscher III at University of Pennsylvania for providing various reagents for this work and John West and Vennu Minhas for helpful discussions.

#### REFERENCES

1. **Abbrink, M., J. A. Ortiz, C. Mark, C. Sanchez, C. Looman, L. Hellman, P. Chambon, and R. Losson.** 2001. Conserved interaction between distinct Kruppel-associated box domains and the transcriptional intermediary factor 1 beta. *Proc. Natl. Acad. Sci. USA* **98**:1422–1426.
2. **Agata, Y., E. Matsuda, and A. Shimizu.** 1999. Two novel Kruppel-associated box-containing zinc-finger proteins, KRAZ1 and KRAZ2, repress transcription through functional interaction with the corepressor KAP-1 (TIF1beta/KRIP-1). *J. Biol. Chem.* **274**:16412–16422.

3. Bellefroid, E. J., D. A. Poncelet, P. J. Lecocq, O. Revelant, and J. A. Martial. 1991. The evolutionarily conserved Kruppel-associated box domain defines a subfamily of eukaryotic multifingered proteins. *Proc. Natl. Acad. Sci. USA* **88**:3608–3612.
4. Bowser, B. S., S. Morris, M. J. Song, R. Sun, and B. Damania. 2006. Characterization of Kaposi's sarcoma-associated herpesvirus (KSHV) K1 promoter activation by Rta. *Virology* **348**:309–327.
5. Brown, H. J., M. J. Song, H. Deng, T. T. Wu, G. Cheng, and R. Sun. 2003. NF- $\kappa$ B inhibits gammaherpesvirus lytic replication. *J. Virol.* **77**:8532–8540.
6. Byun, H., Y. Gwack, S. Hwang, and J. Choe. 2002. Kaposi's sarcoma-associated herpesvirus open reading frame (ORF) 50 transactivates K8 and ORF57 promoters via heterogeneous response elements. *Mol. Cells* **14**:185–191.
7. Carlson, K. A., G. Leisman, J. Limoges, G. D. Pohlman, M. Horiba, J. Buescher, H. E. Gendelman, and T. Ikezu. 2004. Molecular characterization of a putative antiretroviral transcriptional factor, OTK18. *J. Immunol.* **172**:381–391.
8. Carlson, K. A., J. Limoges, G. D. Pohlman, L. Y. Poluektova, D. Langford, E. Masliah, T. Ikezu, and H. E. Gendelman. 2004. OTK18 expression in brain mononuclear phagocytes parallels the severity of HIV-1 encephalitis. *J. Neuroimmunol.* **150**:186–198.
9. Chang, Y., E. Cesarman, M. S. Pessin, F. Lee, J. Culpepper, D. M. Knowles, and P. S. Moore. 1994. Identification of herpesvirus-like DNA sequences in AIDS-associated Kaposi's sarcoma. *Science* **266**:1865–1869.
10. Deng, H., A. Young, and R. Sun. 2000. Auto-activation of the rta gene of human herpesvirus-8/Kaposi's sarcoma-associated herpesvirus. *J. Gen. Virol.* **81**:3043–3048.
11. Duan, W., S. Wang, S. Liu, and C. Wood. 2001. Characterization of Kaposi's sarcoma-associated herpesvirus/human herpesvirus-8 ORF57 promoter. *Arch. Virol.* **146**:403–413.
12. Friedman, J. R., W. J. Fredericks, D. E. Jensen, D. W. Speicher, X. P. Huang, E. G. Neilson, and F. J. Rauscher III. 1996. KAP-1, a novel corepressor for the highly conserved KRAB repression domain. *Genes Dev.* **10**:2067–2078.
13. Gebelein, B., M. Fernandez-Zapico, M. Imoto, and R. Urrutia. 1998. KRAB-independent suppression of neoplastic cell growth by the novel zinc finger transcription factor KS1. *J. Clin. Investig.* **102**:1911–1919.
14. Gebelein, B., and R. Urrutia. 2001. Sequence-specific transcriptional repression by KS1, a multiple-zinc-finger-Kruppel-associated box protein. *Mol. Cell. Biol.* **21**:928–939.
15. Gradoville, L., J. Gerlach, E. Grogan, D. Shedd, S. Nikiforow, C. Metroka, and G. Miller. 2000. Kaposi's sarcoma-associated herpesvirus open reading frame 50/Rta protein activates the entire viral lytic cycle in the HH-B2 primary effusion lymphoma cell line. *J. Virol.* **74**:6207–6212.
16. Gwack, Y., H. J. Baek, H. Nakamura, S. H. Lee, M. Meisterernst, R. G. Roeder, and J. U. Jung. 2003. Principal role of TRAP/mediator and SWI/SNF complexes in Kaposi's sarcoma-associated herpesvirus RTA-mediated lytic reactivation. *Mol. Cell. Biol.* **23**:2055–2067.
17. Gwack, Y., H. Byun, S. Hwang, C. Lim, and J. Choe. 2001. CREB-binding protein and histone deacetylase regulate the transcriptional activity of Kaposi's sarcoma-associated herpesvirus open reading frame 50. *J. Virol.* **75**:1909–1917.
18. Gwack, Y., S. Hwang, C. Lim, Y. S. Won, C. H. Lee, and J. Choe. 2002. Kaposi's sarcoma-associated herpesvirus open reading frame 50 stimulates the transcriptional activity of STAT3. *J. Biol. Chem.* **277**:6438–6442.
19. Gwack, Y., H. Nakamura, S. H. Lee, J. Souvlis, J. T. Yustein, S. Gyi, H.-J. Kung, and J. U. Jung. 2003. Poly(ADP-ribose) polymerase 1 and Ste20-like kinase hKFC act as transcriptional repressors for gamma-2 herpesvirus lytic replication. *Mol. Cell. Biol.* **23**:8282–8294.
20. Hennemann, H., L. Vassen, C. Geisen, M. Eilers, and T. Moroy. 2003. Identification of a novel Kruppel-associated box domain protein, Krim-1, that interacts with c-Myc and inhibits its oncogenic activity. *J. Biol. Chem.* **278**:28799–28811.
21. Hering, T. M., N. H. Kazmi, T. D. Huynh, J. Kollar, L. Xu, A. B. Hunyady, and B. Johnstone. 2004. Characterization and chondrocyte differentiation stage-specific expression of KRAB zinc-finger protein gene ZNF470. *Exp. Cell. Res.* **299**:137–147.
22. Izumiya, Y., S. F. Lin, T. Ellison, L. Y. Chen, C. Izumiya, P. Luciw, and H. J. Kung. 2003. Kaposi's sarcoma-associated herpesvirus K-bZIP is a coregulator of K-Rta: physical association and promoter-dependent transcriptional repression. *J. Virol.* **77**:1441–1451.
23. Jenner, R. G., M. M. Alba, C. Boshoff, and P. Kellam. 2001. Kaposi's sarcoma-associated herpesvirus latent and lytic gene expression as revealed by DNA arrays. *J. Virol.* **75**:891–902.
24. Jheon, A. H., B. Ganss, S. Cheifetz, and J. Sodek. 2001. Characterization of a novel KRAB/C2H2 zinc finger transcription factor involved in bone development. *J. Biol. Chem.* **276**:18282–18289.
25. Katoh, O., T. Oguri, T. Takahashi, S. Takai, Y. Fujiwara, and H. Watanabe. 1998. ZK1, a novel Kruppel-type zinc finger gene, is induced following exposure to ionizing radiation and enhances apoptotic cell death on hematopoietic cells. *Biochem. Biophys. Res. Commun.* **249**:595–600.
26. Kim, S. S., Y. M. Chen, E. O'Leary, R. Witzgall, M. Vidal, and J. V. Bonventre. 1996. A novel member of the RING finger family, KRIP-1, associates with the KRAB-A transcriptional repressor domain of zinc finger proteins. *Proc. Natl. Acad. Sci. USA* **93**:15299–15304.
27. Krishnan, H. H., P. P. Naranatt, M. S. Smith, L. Zeng, C. Bloomer, and B. Chandran. 2004. Concurrent expression of latent and a limited number of lytic genes with immune modulation and antiapoptotic function by Kaposi's sarcoma-associated herpesvirus early during infection of primary endothelial and fibroblast cells and subsequent decline of lytic gene expression. *J. Virol.* **78**:3601–3620.
28. Lan, K., D. A. Kuppers, S. C. Verma, and E. S. Robertson. 2004. Kaposi's sarcoma-associated herpesvirus-encoded latency-associated nuclear antigen inhibits lytic replication by targeting Rta: a potential mechanism for virus-mediated control of latency. *J. Virol.* **78**:6585–6594.
29. Lan, K., D. A. Kuppers, S. C. Verma, N. Sharma, M. Murakami, and E. S. Robertson. 2005. Induction of Kaposi's sarcoma-associated herpesvirus latency-associated nuclear antigen by the lytic transactivator RTA: a novel mechanism for establishment of latency. *J. Virol.* **79**:7453–7465.
30. Lechner, M. S., G. E. Begg, D. W. Speicher, and F. J. Rauscher III. 2000. Molecular determinants for targeting heterochromatin protein 1-mediated gene silencing: direct chromoshadow domain-KAP-1 corepressor interaction is essential. *Mol. Cell. Biol.* **20**:6449–6465.
31. Li, Z., D. Wang, X. Na, S. R. Schoen, E. M. Messing, and G. Wu. 2003. The VHL protein recruits a novel KRAB-A domain protein to repress HIF-1 $\alpha$  transcriptional activity. *EMBO J.* **22**:1857–1867.
32. Liang, Y., J. Chang, S. J. Lynch, D. M. Lukac, and D. Ganem. 2002. The lytic switch protein of KSHV activates gene expression via functional interaction with RBP-J $\kappa$  (CSL), the target of the Notch signaling pathway. *Genes Dev.* **16**:1977–1989.
33. Liang, Y., and D. Ganem. 2004. RBP-J (CSL) is essential for activation of the K14/vGPCR promoter of Kaposi's sarcoma-associated herpesvirus by the lytic switch protein RTA. *J. Virol.* **78**:6818–6826.
34. Liao, G., J. Huang, E. D. Fixman, and S. D. Hayward. 2005. The Epstein-Barr virus replication protein BBLF2/3 provides an origin-tethering function through interaction with the zinc finger DNA binding protein ZBRK1 and the KAP-1 corepressor. *J. Virol.* **79**:245–256.
35. Liao, W., Y. Tang, S. F. Lin, H. J. Kung, and C. Z. Giam. 2003. K-bZIP of Kaposi's sarcoma-associated herpesvirus/human herpesvirus 8 (KSHV/HHV-8) binds KSHV/HHV-8 Rta and represses Rta-mediated transactivation. *J. Virol.* **77**:3809–3815.
36. Lin, S. F., D. R. Robinson, G. Miller, and H. J. Kung. 1999. Kaposi's sarcoma-associated herpesvirus encodes a bZIP protein with homology to BZLF1 of Epstein-Barr virus. *J. Virol.* **73**:1909–1917.
37. Looman, C., M. Abrink, C. Mark, and L. Hellman. 2002. KRAB zinc finger proteins: an analysis of the molecular mechanisms governing their increase in numbers and complexity during evolution. *Mol. Biol. Evol.* **19**:2118–2130.
38. Looman, C., L. Hellman, and M. Abrink. 2004. A novel Kruppel-associated box identified in a panel of mammalian zinc finger proteins. *Mamm. Genome* **15**:35–40.
39. Looman, C., C. Mark, M. Abrink, and L. Hellman. 2003. MZF6D, a novel KRAB zinc-finger gene expressed exclusively in meiotic male germ cells. *DNA Cell Biol.* **22**:489–496.
40. Lorenz, P., D. Koczan, and H. J. Thiesen. 2001. Transcriptional repression mediated by the KRAB domain of the human C2H2 zinc finger protein Kox1/ZNF10 does not require histone deacetylation. *Biol. Chem.* **382**:637–644.
41. Lukac, D. M., L. Garibyan, J. R. Kirshner, D. Palmeri, and D. Ganem. 2001. DNA binding by Kaposi's sarcoma-associated herpesvirus lytic switch protein is necessary for transcriptional activation of two viral delayed early promoters. *J. Virol.* **75**:6786–6799.
42. Lukac, D. M., J. R. Kirshner, and D. Ganem. 1999. Transcriptional activation by the product of open reading frame 50 of Kaposi's sarcoma-associated herpesvirus is required for lytic viral reactivation in B cells. *J. Virol.* **73**:9348–9361.
43. Lukac, D. M., R. Renne, J. R. Kirshner, and D. Ganem. 1998. Reactivation of Kaposi's sarcoma-associated herpesvirus infection from latency by expression of the ORF 50 transactivator, a homolog of the EBV R protein. *Virology* **252**:304–312.
44. Margolin, J. F., J. R. Friedman, W. K. Meyer, H. Vissing, H. J. Thiesen, and F. J. Rauscher III. 1994. Kruppel-associated boxes are potent transcriptional repression domains. *Proc. Natl. Acad. Sci. USA* **91**:4509–4513.
45. Mark, C., M. Abrink, and L. Hellman. 1999. Comparative analysis of KRAB zinc finger proteins in rodents and man: evidence for several evolutionarily distinct subfamilies of KRAB zinc finger genes. *DNA Cell Biol.* **18**:381–396.
46. Matsumura, S., Y. Fujita, E. Gomez, N. Tanese, and A. C. Wilson. 2005. Activation of the Kaposi's sarcoma-associated herpesvirus major latency locus by the lytic switch protein RTA (ORF50). *J. Virol.* **79**:8493–8505.
47. Medugno, L., F. Florio, R. De Cegli, M. Grosso, A. Lupo, P. Costanzo, and P. Izzo. 2005. The Kruppel-like zinc-finger protein ZNF224 represses aldolase A gene transcription by interacting with the KAP-1 co-repressor protein. *Gene* **359**:35–43.
48. Moosmann, P., O. Georgiev, B. Le Douarin, J. P. Bourquin, and W. Schaffner. 1996. Transcriptional repression by RING finger protein TIF1

- beta that interacts with the KRAB repressor domain of KOX1. *Nucleic Acids Res.* **24**:4859–4867.
49. Moosmann, P., O. Georgiev, H. J. Thiesen, M. Hagmann, and W. Schaffner. 1997. Silencing of RNA polymerases II and III-dependent transcription by the KRAB protein domain of KOX1, a Kruppel-type zinc finger factor. *Biol. Chem.* **378**:669–677.
  50. Nakamura, H., M. Lu, Y. Gwack, J. Souvlis, S. L. Zeichner, and J. U. Jung. 2003. Global changes in Kaposi's sarcoma-associated virus gene expression patterns following expression of a tetracycline-inducible Rta transactivator. *J. Virol.* **77**:4205–4220.
  51. Nielsen, A. L., P. Jorgensen, T. Lerouge, M. Cervino, P. Chambon, and R. Losson. 2004. Nizp1, a novel multitype zinc finger protein that interacts with the NSD1 histone lysine methyltransferase through a unique C2HR motif. *Mol. Cell. Biol.* **24**:5184–5196.
  52. Nielsen, A. L., J. A. Ortiz, J. You, M. Oulad-Abdelghani, R. Khechumian, A. Gansmuller, P. Chambon, and R. Losson. 1999. Interaction with members of the heterochromatin protein 1 (HP1) family and histone deacetylation are differentially involved in transcriptional silencing by members of the TIF1 family. *EMBO J.* **18**:6385–6395.
  53. Ogryzko, V. V., R. L. Schiltz, V. Russanova, B. H. Howard, and Y. Nakatani. 1996. The transcriptional coactivators p300 and CBP are histone acetyltransferases. *Cell* **87**:953–959.
  54. Pearce, M., S. Matsumura, and A. C. Wilson. 2005. Transcripts encoding K12, v-FLIP, v-cyclin, and the microRNA cluster of Kaposi's sarcoma-associated herpesvirus originate from a common promoter. *J. Virol.* **79**:14457–14464.
  55. Peng, H., G. E. Begg, S. L. Harper, J. R. Friedman, D. W. Speicher, and F. J. Rauscher III. 2000. Biochemical analysis of the Kruppel-associated box (KRAB) transcriptional repression domain. *J. Biol. Chem.* **275**:18000–18010.
  56. Peng, H., G. E. Begg, D. C. Schultz, J. R. Friedman, D. E. Jensen, D. W. Speicher, and F. J. Rauscher III. 2000. Reconstitution of the KRAB-KAP-1 repressor complex: a model system for defining the molecular anatomy of RING-B box-coiled-coil domain-mediated protein-protein interactions. *J. Mol. Biol.* **295**:1139–1162.
  57. Peng, H., L. Zheng, W. H. Lee, J. J. Rux, and F. J. Rauscher III. 2002. A common DNA-binding site for SZF1 and the BRCA1-associated zinc finger protein, ZBRK1. *Cancer Res.* **62**:3773–3781.
  58. Rousseau-Merck, M. F., D. Koczan, I. Legrand, S. Moller, S. Autran, and H. J. Thiesen. 2002. The KOX zinc finger genes: genome wide mapping of 368 ZNF PAC clones with zinc finger gene clusters predominantly in 23 chromosomal loci are confirmed by human sequences annotated in Ensembl. *Cytogenet. Genome Res.* **98**:147–153.
  59. Ryan, R. F., D. C. Schultz, K. Ayyanathan, P. B. Singh, J. R. Friedman, W. J. Fredericks, and F. J. Rauscher III. 1999. KAP-1 corepressor protein interacts and colocalizes with heterochromatic and euchromatic HP1 proteins: a potential role for Kruppel-associated box-zinc finger proteins in heterochromatin-mediated gene silencing. *Mol. Cell. Biol.* **19**:4366–4378.
  60. Sadowski, I. 1995. Uses for GAL4 expression in mammalian cells. *Genet. Eng. (New York)* **17**:119–148.
  61. Sakakibara, S., K. Ueda, J. Chen, T. Okuno, and K. Yamanishi. 2001. Octamer-binding sequence is a key element for the autoregulation of Kaposi's sarcoma-associated herpesvirus ORF50/Lyta gene expression. *J. Virol.* **75**:6894–6900.
  62. Sarid, R., O. Flore, R. A. Bohenzky, Y. Chang, and P. S. Moore. 1998. Transcription mapping of the Kaposi's sarcoma-associated herpesvirus (human herpesvirus 8) genome in a body cavity-based lymphoma cell line (BC-1). *J. Virol.* **72**:1005–1012.
  63. Schultz, D. C., K. Ayyanathan, D. Negorev, G. G. Maul, and F. J. Rauscher III. 2002. SETDB1: a novel KAP-1-associated histone H3, lysine 9-specific methyltransferase that contributes to HP1-mediated silencing of euchromatic genes by KRAB zinc-finger proteins. *Genes Dev.* **16**:919–932.
  64. Schultz, D. C., J. R. Friedman, and F. J. Rauscher III. 2001. Targeting histone deacetylase complexes via KRAB-zinc finger proteins: the PHD and bromodomains of KAP-1 form a cooperative unit that recruits a novel isoform of the Mi-2 $\alpha$  subunit of NuRD. *Genes Dev.* **15**:428–443.
  65. Seaman, W. T., D. Ye, R. X. Wang, E. E. Hale, M. Weisse, and E. B. Quinlivan. 1999. Gene expression from the ORF50/K8 region of Kaposi's sarcoma-associated herpesvirus. *Virology* **263**:436–449.
  66. Shmueli, O., S. Horn-Saban, V. Chalifa-Caspi, M. Shmoish, R. Ophir, H. Benjamin-Rodrig, M. Safran, E. Domany, and D. Lancet. 2003. GeneNote: whole genome expression profiles in normal human tissues. *C. R. Biol.* **326**:1067–1072.
  67. Skapek, S. X., D. Jansen, T. F. Wei, T. McDermott, W. Huang, E. N. Olson, and E. Y. Lee. 2000. Cloning and characterization of a novel Kruppel-associated box family transcriptional repressor that interacts with the retinoblastoma gene product, RB. *J. Biol. Chem.* **275**:7212–7223.
  68. Song, M. J., H. J. Brown, T. T. Wu, and R. Sun. 2001. Transcription activation of polyadenylated nuclear RNA by Rta in human herpesvirus 8/Kaposi's sarcoma-associated herpesvirus. *J. Virol.* **75**:3129–3140.
  69. Song, M. J., X. Li, H. J. Brown, and R. Sun. 2002. Characterization of interactions between RTA and the promoter of polyadenylated nuclear RNA in Kaposi's sarcoma-associated herpesvirus/human herpesvirus 8. *J. Virol.* **76**:5000–5013.
  70. Sun, R., S. F. Lin, L. Gradoville, Y. Yuan, F. Zhu, and G. Miller. 1998. A viral gene that activates lytic cycle expression of Kaposi's sarcoma-associated herpesvirus. *Proc. Natl. Acad. Sci. USA* **95**:10866–10871.
  71. Takase, K., T. Ohtsuki, O. Migita, M. Toru, T. Inada, K. Yamakawa-Kobayashi, and T. Arinami. 2001. Association of ZNF74 gene genotypes with age-at-onset of schizophrenia. *Schizophr. Res.* **52**:161–165.
  72. Takashima, H., H. Nishio, H. Wakao, M. Nishio, K. Koizumi, A. Oda, T. Koike, and K. Sawada. 2001. Molecular cloning and characterization of a KRAB-containing zinc finger protein, ZNF317, and its isoforms. *Biochem. Biophys. Res. Commun.* **288**:771–779.
  73. Tian, Y., G. J. Breedveld, S. Huang, B. A. Oostra, P. Heutink, and W. H. Lo. 2002. Characterization of ZNF333, a novel double KRAB domain containing zinc finger gene on human chromosome 19p13.1. *Biochim. Biophys. Acta* **1577**:121–125.
  74. Tommerup, N., and H. Vissing. 1995. Isolation and fine mapping of 16 novel human zinc finger-encoding cDNAs identify putative candidate genes for developmental and malignant disorders. *Genomics* **27**:259–264.
  75. Urrutia, R. 2003. KRAB-containing zinc-finger repressor proteins. *Genome Biol.* **4**:231.
  76. Vieira, J., and P. M. O'Hearn. 2004. Use of the red fluorescent protein as a marker of Kaposi's sarcoma-associated herpesvirus lytic gene expression. *Virology* **325**:225–240.
  77. Vissing, H., W. K. Meyer, L. Aagaard, N. Tommerup, and H. J. Thiesen. 1995. Repression of transcriptional activity by heterologous KRAB domains present in zinc finger proteins. *FEBS Lett.* **369**:153–157.
  78. Wang, J., J. Zhang, L. Zhang, W. Harrington, Jr., J. T. West, and C. Wood. 2005. Modulation of human herpesvirus 8/Kaposi's sarcoma-associated herpesvirus replication and transcription activator transactivation by interferon regulatory factor 7. *J. Virol.* **79**:2420–2431.
  79. Wang, S., S. Liu, M. Wu, Y. Geng, and C. Wood. 2001. Kaposi's sarcoma-associated herpesvirus/human herpesvirus-8 ORF50 gene product contains a potent C-terminal activation domain which activates gene expression via a specific target sequence. *Arch. Virol.* **146**:1415–1426.
  80. Wang, S., S. Liu, M. H. Wu, Y. Geng, and C. Wood. 2001. Identification of a cellular protein that interacts and synergizes with the RTA (ORF50) protein of Kaposi's sarcoma-associated herpesvirus in transcriptional activation. *J. Virol.* **75**:11961–11973.
  81. Wang, S. E., F. Y. Wu, Y. Yu, and G. S. Hayward. 2003. CCAAT/enhancer-binding protein-alpha is induced during the early stages of Kaposi's sarcoma-associated herpesvirus (KSHV) lytic cycle reactivation and together with the KSHV replication and transcription activator (RTA) cooperatively stimulates the viral RTA, MTA, and PAN promoters. *J. Virol.* **77**:9590–9612.
  82. Witzgall, R., E. O'Leary, A. Leaf, D. Onaldi, and J. V. Bonventre. 1994. The Kruppel-associated box-A (KRAB-A) domain of zinc finger proteins mediates transcriptional repression. *Proc. Natl. Acad. Sci. USA* **91**:4514–4518.
  83. Yang, J. J. 2003. A novel zinc finger protein, ZZAPK, interacts with ZAK and stimulates the ZAK-expressing cells re-entering the cell cycle. *Biochem. Biophys. Res. Commun.* **301**:71–77.
  84. Yi, Z., Y. Li, W. Ma, D. Li, C. Zhu, J. Luo, Y. Wang, X. Huang, W. Yuan, M. Liu, and X. Wu. 2004. A novel KRAB zinc-finger protein, ZNF480, expresses in human heart and activates transcriptional activities of AP-1 and SRE. *Biochem. Biophys. Res. Commun.* **320**:409–415.
  85. Yu, Y., S. E. Wang, and G. S. Hayward. 2005. The KSHV immediate-early transcription factor RTA encodes ubiquitin E3 ligase activity that targets IRF7 for proteasome-mediated degradation. *Immunity* **22**:59–70.
  86. Zeleznik-Le, N. J., A. M. Harden, and J. D. Rowley. 1994. 11q23 translocations split the "AT-hook" cruciform DNA-binding region and the transcriptional repression domain from the activation domain of the mixed-lineage leukemia (MLL) gene. *Proc. Natl. Acad. Sci. USA* **91**:10610–10614.
  87. Zheng, L., H. Pan, S. Li, A. Flesken-Nikitin, P. L. Chen, T. G. Boyer, and W. H. Lee. 2000. Sequence-specific transcriptional corepressor function for BRCA1 through a novel zinc finger protein, ZBRK1. *Mol. Cell* **6**:757–768.
  88. Ziegelbauer, J., A. Grundhoff, and D. Ganem. 2006. Exploring the DNA binding interactions of the Kaposi's sarcoma-associated herpesvirus lytic switch protein by selective amplification of bound sequences in vitro. *J. Virol.* **80**:2958–2967.